

# Tunable Laser Diode System for Noninvasive Blood Glucose Measurements

JONATHON T. OLESBERG,\* MARK A. ARNOLD, CARMEN MERMELSTEIN, JOHANNES SCHMITZ, and JOACHIM WAGNER

*Optical Science and Technology Center and the Department of Chemistry, 100 IATL, University of Iowa, Iowa City, Iowa 52242 (J.T.O., M.A.A.); and Fraunhofer-Institut fuer Angewandte Festkoerperphysik (IAF), Tullastrasse 72, D-79108, Freiburg, Germany (C.M., J.S., J.W.)*

Optical sensing of glucose would allow more frequent monitoring and tighter glucose control for people with diabetes. The key to a successful optical noninvasive measurement of glucose is the collection of an optical spectrum with a very high signal-to-noise ratio in a spectral region with significant glucose absorption. Unfortunately, the optical throughput of skin is low due to absorption and scattering. To overcome these difficulties, we have developed a high-brightness tunable laser system for measurements in the 2.0–2.5  $\mu\text{m}$  wavelength range. The system is based on a 2.3  $\mu\text{m}$  wavelength, strained quantum-well laser diode incorporating GaInAsSb wells and AlGaAsSb barrier and cladding layers. Wavelength control is provided by coupling the laser diode to an external cavity that includes an acousto-optic tunable filter. Tuning ranges of greater than 110 nm have been obtained. Because the tunable filter has no moving parts, scans can be completed very quickly, typically in less than 10 ms. We describe the performance of the present laser system and avenues for extending the tuning range beyond 400 nm.

Index Headings: Glucose; Tunable laser; Near-infrared spectroscopy; Noninvasive sensing; Acousto-optic tunable filter; AOTF; External cavity; GaInAsSb; Diabetes.

## INTRODUCTION

The benefits of tight glycemic control in people with diabetes are well-documented.<sup>1–3</sup> Hyperglycemia over extended periods is the primary cause of the severe complications associated with diabetes, including premature death, blindness, kidney failure, amputations, heart disease, and stroke. Effective glycemic control requires frequent blood glucose monitoring to provide the information needed to administer the proper amount of insulin while avoiding hypoglycemia.

Frequent blood glucose monitoring would be more widely practiced with the availability of an analytical system that operates in a manner that is accurate, painless, sample-free, and easily implemented by the diabetic patient during his/her normal daily routine. State-of-the-art glucose monitoring technology falls considerably short of these requirements. Current test-strip technology requires a blood sample for each measurement. The pain associated with such measurements can inhibit frequent monitoring, especially in children. Frequent monitoring is also discouraged by the need to handle and dispose of the blood sample and by the difficulty of implementing the test in social settings. Current industry-wide efforts to reduce the size of the required blood sample and to shorten the analysis time are beneficial, but they do not ad-

dress the fundamental limitations of an invasive procedure.

Noninvasive optical sensing of glucose has been proposed by many research groups for the frequent and painless measurement of glucose in people with diabetes.<sup>4</sup> The concept is to pass a selected band of near-infrared radiation through a vascular region of the body and extract the glucose concentration from the resulting spectral information. Near-infrared spectroscopy is a promising approach for noninvasive sensing because of the unique near-infrared absorption spectrum of glucose and the significant penetration of near-infrared light into human tissue.

One of the primary difficulties with performing optical absorption measurements in skin is the low optical throughput. In addition to the strong water absorption (0.9 AU/mm at 2.2  $\mu\text{m}$  wavelength), skin is highly scattering. In separate noninvasive measurements using conventional Fourier transform infrared (FT-IR) instrumentation,<sup>5</sup> the peak transmission through a sample with an effective aqueous path length of 0.6 mm is typically 0.1–1.0%. In order to maximize the signal-to-noise ratio of the measurement, it is helpful to have the brightest source possible. We presently use 50 W tungsten filament bulbs that operate at 3050 K. Although higher power bulbs can be obtained, their brightness (optical power per unit radiating area) does not increase with power.

Laser diodes would be a very useful tool for tissue spectroscopy because of their brightness, which enables large optical powers to be collected onto a small, low noise detector. Laser diodes, being solid-state devices, could lead to more compact and rugged spectrometers compared to a system that requires a sensitive interferometer. In order to be useful for noninvasive spectroscopy, however, a laser diode system must be capable of acquiring a spectrum consisting of measurements at a number of wavelengths. The need for a spectrum rather than measurements at one or two discrete wavelengths is a consequence of the broad and highly overlapped nature of near-infrared absorption bands. The need for measurements over a range of wavelengths is illustrated in Fig. 1, which shows the absorptivity spectrum of glucose compared with that of several other biomolecules. The glucose absorption spectrum is unique, but it is highly overlapped with the other spectra. Disentangling the glucose signal from a composite spectrum can be accomplished with multivariate techniques, such as partial least-squares regression. Multivariate techniques inherently require measurements at a number of wavelengths.

Received 8 March 2005; accepted 12 October 2005.

\* Author to whom correspondence should be sent. E-mail: jonathon-olesberg@uiowa.edu.

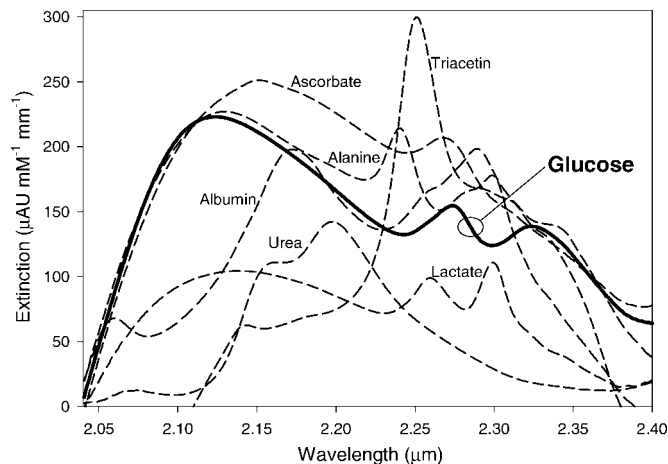


FIG. 1. Absorptivity of glucose and a sampling of other biomolecules in the 2.0–2.5  $\mu\text{m}$  wavelength range. The glucose absorptivity spectrum is unique, but exhibits significant overlap with the absorptivity spectra of other biomolecules.

There are at least two ways to collect a spectrum using a laser diode. The first is to use a set of diodes, each operating at a fixed wavelength. To be useful for transcutaneous spectroscopy, however, this would require at least 12–18 devices, each of which is locked at a particular wavelength. This arrangement represents a straightforward but cumbersome solution. The second way to obtain a spectrum is to use a single emitter whose wavelength is tunable.

With regards to spectroscopy, tunable laser diodes have been used across both near-infrared<sup>6–10</sup> and mid-infrared<sup>11–13</sup> wavelengths. The vast majority of spectroscopic work performed using tunable laser diodes has been directed at gas sensing. The requirements for noninvasive aqueous sensing, however, are very different from those of gas sensing because of the difference between gas-phase and condensed-phase absorption spectra. Gas-phase absorption spectra comprise several sharp features that correspond to the rotational modes of the gas molecule. By contrast, the aqueous glucose spectrum is composed of features with widths of 25–100 nm ( $50\text{--}200\text{ cm}^{-1}$ ). A tunable laser diode system designed to measure gas will typically scan across a single rotation line to quantify the species (0.1 nm of tuning). For aqueous spectra, however, much broader tunability is required (250–400 nm, or  $500\text{--}800\text{ cm}^{-1}$ ). While gas sensing requires very narrow laser linewidths to resolve the sharp features, narrow linewidths are not necessary for aqueous sensing. The typical spectral resolution utilized in our transcutaneous measurements is 8 nm ( $16\text{ cm}^{-1}$ ).<sup>5</sup>

Several tuning strategies have been employed with tunable laser diode systems. The most convenient strategies involve only electronic wavelength control. For example, current can be injected into regions of the device in order to modify the index of refraction of the material, which leads to a shift in wavelength. Alternatively, the current used to drive the device can be ramped in order to rapidly vary the device temperature, which causes a shift in wavelength. Both of these approaches provide tunability over narrow wavelength bands, which is sufficient for gas sensing but not for aqueous spectroscopy. Tuning can also be achieved by directly modifying the temperature

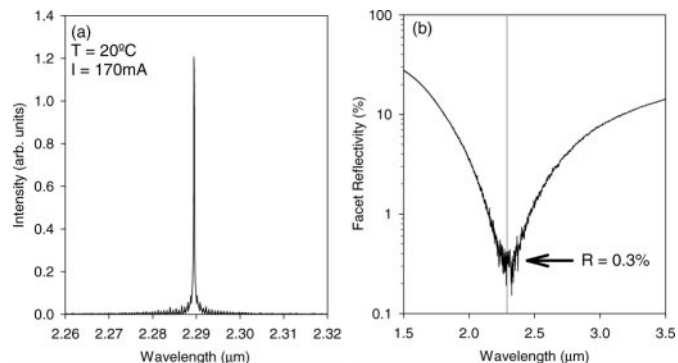


FIG. 2. (a) Free lasing spectrum of the anti-reflection-coated laser diode operating just above threshold. (b) Reflectivity of the anti-reflection-coated facet. The vertical line shows the free lasing wavelength of the device.

of the device heat-sink, but this provides limited tuning range and is slow. Recently, wide tuning ranges have been obtained by subjecting the laser device to high-pressures, but it is unclear whether this can be accomplished in a practical manner without damaging the devices.<sup>14–16</sup> An additional strategy is to employ an external cavity, which can provide a wider tuning range than electrical or temperature tuning. Tuning ranges of up to 242 nm ( $1170\text{ cm}^{-1}$ ) have been reported in the literature.<sup>17,18</sup> External cavity systems at longer wavelengths have demonstrated tuning ranges from 3.40–3.68  $\mu\text{m}$  ( $224\text{ cm}^{-1}$ ).<sup>19,20</sup>

## EXPERIMENTAL

The work described here was performed with coated Fabry–Perot laser diodes fabricated at the Fraunhofer Institute for Applied Solid-State Physics. These devices are based on an active region with three strained  $\text{Ga}_{0.70}\text{In}_{0.30}\text{As}_{0.06}\text{Sb}_{0.94}$  quantum wells,  $\text{Al}_{0.28}\text{Ga}_{0.72}\text{As}_{0.02}\text{Sb}_{0.98}$  barriers and separate confinement regions, and  $\text{Al}_{0.85}\text{Ga}_{0.15}\text{As}_{0.07}\text{Sb}_{0.93}$  waveguide cladding layers.<sup>21–24</sup> The devices were 1 mm long ridge waveguide lasers with a ridge width of 16  $\mu\text{m}$ . The devices were mounted epilayer-side down on a copper C-mount heat-sink. The optimal device for wavelength tuning had a 95% high-reflective coating on one end and a 0.3% anti-reflection coating on the other. The device operates with a natural wavelength of 2.29  $\mu\text{m}$  with a threshold current of 150 mA at a heat-sink temperature of 20  $^{\circ}\text{C}$ . Figure 2a shows the natural lasing spectrum of the device at a current of 170 mA. Shown in Fig. 2b is a measurement of the reflectivity of the anti-reflection coated facet, which is designed to reach a minimum reflectivity at the natural lasing wavelength.

The laser diode was mounted on a thermoelectric temperature-controlled mount and coupled into an external cavity arrangement. A photograph and simplified schematic of the system are shown in Fig. 3. The laser output from the facet with the anti-reflection coating was collected with a high numeric aperture asphere ( $\text{NA} = 0.55$  and  $f = 4.51\text{ mm}$ ) and imaged onto a flat end-mirror (which also serves as an output coupler) 20 cm away. A beam-splitter could optionally be inserted in the cavity in order to pick off a small portion of the beam during alignment. An acousto-optic tunable filter (AOTF) was placed

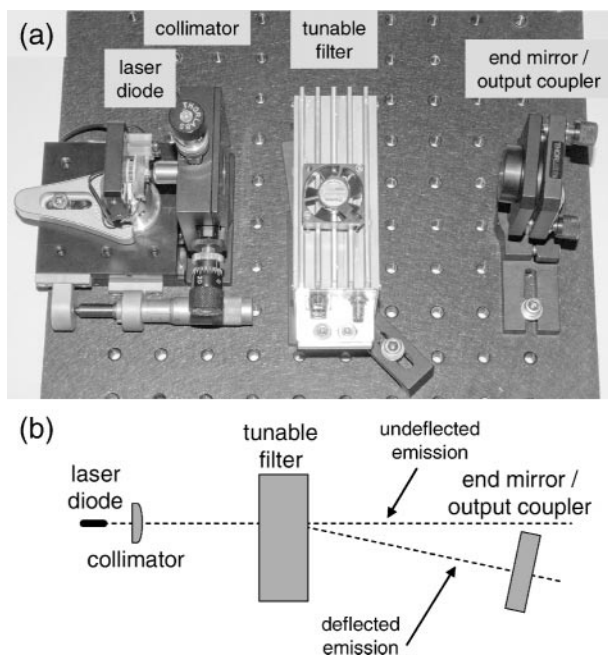


FIG. 3. (a) Photograph of the present external cavity system, and (b) a simplified schematic.

between the collimating lens and end-mirror. The tunable filter (Brimrose Corp.) is based on a temperature-stabilized  $\text{TeO}_2$  crystal and optimized for the 2.0–2.5  $\mu\text{m}$  wavelength range with a pass-band width of 12 nm and a diffraction efficiency greater than 50%. The tunable filter causes a  $6^\circ$  horizontal deflection of the selected wavelength band, which requires that the end-mirror be rotated by  $6^\circ$  off-normal with respect to the output from the laser diode. The tunable filter is driven by a custom-designed radio-frequency (RF) driver based on an Analog Devices AD9854 direct-digital-synthesis signal generator chip. The synthesizer chip is controlled by a microcontroller, which programs the synthesizer to generate a chirped sine wave with frequencies running from 40–45 MHz. The chirp is amplified by a 4 watt RF power amplifier and delivered to the tunable filter. A small portion of the system output is picked off using a pellicle beam splitter and delivered to an extended-wavelength InGaAs detector to provide a reference channel. The system as a whole is mounted on a 12 in. optical breadboard so that the system can be moved and positioned as a unit.

## RESULTS AND DISCUSSION

The present system is capable of tuning over a wavelength range of more than 110 nm ( $220\text{ cm}^{-1}$ ), as is illustrated by the spectra in Fig. 4, which were collected at a series of fixed RF drive frequencies using an FT-IR spectrometer. The external cavity system begins to lase at a threshold current of 105 mA and obtains optimal tunability at a drive current of 200 mA. At higher currents, the output power continues to increase although the tuning range narrows slightly due to carrier loss to internal cavity lasing. Note, however, from the schematic in Fig. 3b, that the internal lasing signal is not collinear with the external cavity output and can be eliminated with a beam-stop. An external cavity utilizing a grating in the Littrow configuration has also been employed. The grat-

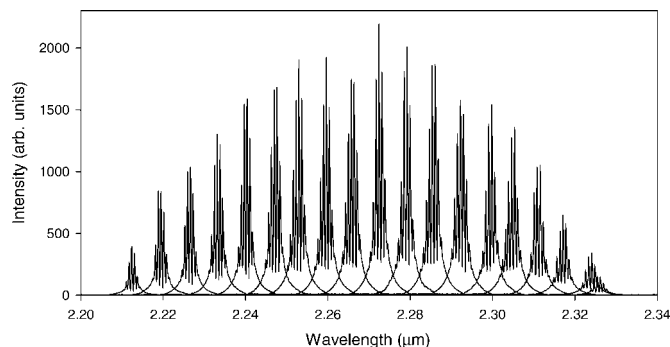


FIG. 4. Tuning spectra obtained with the present external cavity system. The fringes are due to feedback from the internal laser diode cavity.

ing-based external cavity had the same threshold current and wavelength tuning range as the AOTF-based system.

With a 90% reflective external cavity output coupler, the optical power at 200 mA is 0.5 mW at the center of the tuning range. Powers of several milliwatts should be obtainable with improved anti-reflection coatings and waveguide geometries. Optical power levels as high as 1 watt have been obtained with shorter wavelength near-infrared external cavity systems.<sup>25</sup> The optical power presently available for our noninvasive glucose work originates from a tungsten filament. The integrated radiant power from this broad-band source collected onto the detector over the 2.0–2.5  $\mu\text{m}$  band is approximately 0.05 mW. Thus, the present 0.5 mW from the tunable laser system represents a factor of 10 improvement in available signal with respect to the broadband source.

In Fig. 4, fringes are visible in each of the lasing spectra. These fringes are due to significant feedback from the anti-reflection-coated facet of the device. The presence of the fringes indicates that the laser is operating in a coupled-cavity regime, which is undesirable.<sup>26–28</sup> The coupling of the internal and external cavities can be reduced by decreasing the feedback from the anti-reflection-coated facet.

Spectra of four chemical components were measured using the tunable laser system and an FT-IR spectrometer to test the tunable laser system's ability to resolve spectral features of glucose and other biomolecules. Solutions of glucose, urea, and acetate were measured in a 1 mm path length cuvette and referenced to water. Absorbance spectra for the solutions are shown in Fig. 5 for measurements made using the tunable laser system and a Nicolet Nexus 670 FT-IR spectrometer. Spectra collected using the FT-IR spectrometer were obtained from 128 coadded interferograms (60 s collection time) with  $16\text{ cm}^{-1}$  resolution using a thermoelectrically cooled, extended wavelength InGaAs detector. A band pass filter was placed before the detector to limit the spectral range to the 2.0–2.5  $\mu\text{m}$  wavelength band. The spectra collected using the tunable laser are the average of 2000 individual scans collected over 60 s. Thermoelectrically cooled InGaAs detectors were used for signal and reference channels.

The spectra recorded using the two systems are very similar in shape and magnitude. Vertical shifts in absorbance spectra are common in the 2.0–2.5  $\mu\text{m}$  wavelength range due to the strong temperature dependence of water absorption and are not analytically significant. Solution

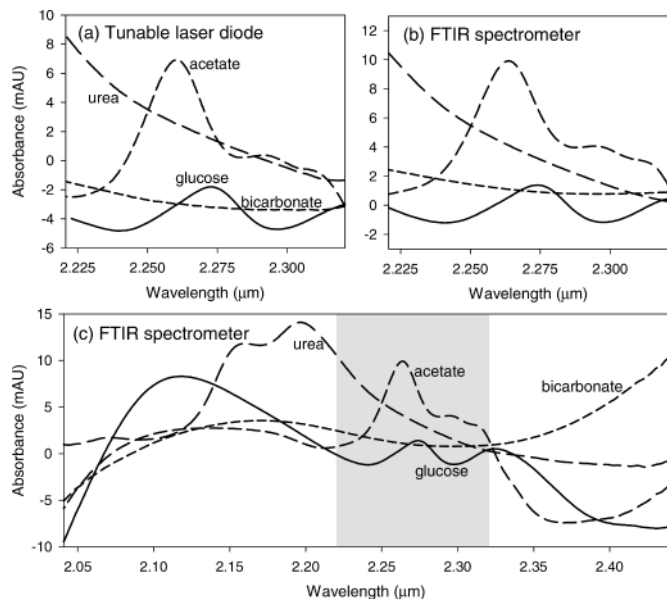


FIG. 5. Absorbance spectra of four analytes measured with (a) the present tunable laser diode spectrometer and (b) an FT-IR spectrometer. (c) The absorbance spectra measured with an FT-IR spectrometer over a wider spectral range. The highlighted region is the portion of the spectra shown above. Note that vertical shifts are common in this wavelength range and are not analytically significant.

temperatures were not controlled during these measurements.

The present tunability of the system is sufficient for *in vitro* quantification of biological analytes such as glucose in moderately complex samples (e.g., for quantification of glucose in interstitial fluid or clear effluent from a bioreactor). However, our experience with *in vivo* measurements indicates that a wider spectral range is required for transcutaneous glucose measurements. Based on our preliminary work with animal models,<sup>5</sup> we estimate that a minimum useful tuning range of 250 nm is required for *in vivo* tissue measurements, whereas 400 nm would be ideal.

The tuning range that can be obtained with an external cavity system depends primarily on three factors: the width of the gain spectrum of the laser diode, the effective reflectivity provided by the external cavity, and the reflectivity of the laser diode facet. The gain spectrum of the laser diode broadens with increasing drive current until the device reaches lasing threshold based on feedback from the front facet. In order to maximize the tunability of the system, the reflectivity from the front facet of the diode needs to be minimized while the amount of light coupled back into the device from the external cavity needs to be maximized.

We have performed calculations of the gain spectrum of the triple-quantum-well material using 14-band  $\mathbf{K}\cdot\mathbf{p}$  theory. This formalism has been used extensively in the past to model the optical and electrical characteristics of near- and mid-infrared quantum wells and superlattices.<sup>29–35</sup> The calculated modal gain spectrum of the device is shown in Fig. 6 for quantum-well-carrier densities of  $3.5\text{--}5.5 \times 10^{17} \text{ cm}^{-3}$ . Also shown in the figure are the threshold gain required for operation with the existing external cavity ( $\gamma_{\text{external}}$ ) and the threshold gain for lasing based on the 0.3% reflectivity of the front device facet

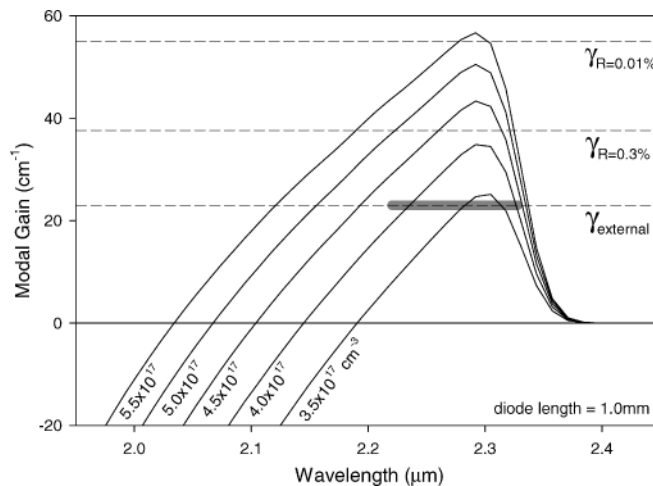


FIG. 6. Gain spectra for the triple-quantum-well laser diode calculated using 14-band  $\mathbf{K}\cdot\mathbf{p}$  theory for a series of carrier densities.  $\gamma_{\text{external}}$  is the gain required for lasing with the external cavity.  $\gamma_{R=0.3\%}$  and  $\gamma_{R=0.01\%}$  are the gains required for lasing without the external cavity with front facet reflectivities of 0.3% and 0.01%, respectively.

( $\gamma_{R=0.3\%}$ ). The threshold gain for lasing off the internal cavity ( $\gamma_{R=0.3\%}$ ) was calculated based on the cavity length, facet reflectivities, and previously measured values for internal loss.<sup>21</sup> Threshold gain for the external cavity ( $\gamma_{\text{external}}$ ) was calculated from  $\gamma_{R=0.3\%}$  and the difference in threshold current for operation with and without the external cavity.

The diode will begin to lase based on feedback from the front facet at a carrier density at which the modal gain exceeds  $\gamma_{R=0.3\%}$ , which in the present device occurs at a carrier density of  $4.2 \times 10^{17} \text{ cm}^{-3}$ . The tuning range that can be obtained with the external cavity can then be calculated by examining the spectral range over which the gain curve for this carrier density exceeds  $\gamma_{\text{external}}$ . The estimated tuning range for the present devices, which is shown in the figure with a gray bar, matches the experimental results.

Two types of modifications to the laser device will extend the tuning range that can be obtained. The first type of modification involves improvements that allow for more efficient coupling of the laser emission back into the device. Wagner et al. have recently reported improved clad designs that reduce the spatial divergence of the laser emission, which allows for higher-efficiency coupling of the emission back into the device and reduction of  $\gamma_{\text{external}}$ .<sup>36,37</sup>

The other type of modification that can be used to extend the tuning range involves suppressing feedback from the front facet of the device. This can be done by improving the efficiency of the anti-reflection coating applied to the facet, by shortening the laser diode, or by utilizing a curved or angled stripe geometry.<sup>38–42</sup> In principle, reflectivities as low as  $10^{-6}$  can be obtained by combining a curved stripe geometry and an anti-reflection coating.<sup>38</sup> Reducing the reflectivity of the front facet to  $10^{-4}$  would increase the threshold gain for internal lasing to  $55 \text{ cm}^{-1}$ , which is shown by the line labeled  $\gamma_{R=0.01\%}$  in Fig. 6. This would allow operation at a carrier density greater than  $5 \times 10^{17} \text{ cm}^{-3}$  and provide tuning from  $2.12\text{--}2.34 \mu\text{m}$  ( $220 \text{ nm}$ , or  $440 \text{ cm}^{-1}$ ). By combin-

ing a reflectivity of  $10^{-4}$  with a shortened laser diode (0.5 mm), the tuning range can be extended well beyond 400 nm, which will be ample for noninvasive sensing.

## CONCLUSION

We report the initial development of a tunable laser diode spectroscopy system designed for the measurement of glucose in *in vivo* transcutaneous spectra. The high-brightness source provides 0.5 mW of power tunable over the 2.21–2.33  $\mu\text{m}$  (4300–4520  $\text{cm}^{-1}$ ) range. Further improvements designed to reduce the optical feedback from the anti-reflection-coated facet will extend the tuning range. Tuning ranges as wide as 400 nm are expected for optimized laser diodes. These capabilities will make the system a highly attractive platform for near-infrared spectroscopy in high optical density samples.

## ACKNOWLEDGMENTS

This research was supported by grants from the National Institute of Diabetes and Digestive and Kidney Diseases of the National Institutes of Health (DK-60657 and DK-02925).

1. Diabetes Control and Complications Trial Research Group, "The effect of intensive treatment of diabetes on the development and progression of long-term complications in insulin-dependent diabetes mellitus", *N. Engl. J. Med.* **329**, 977 (1993).
2. *Diabetes in America*, NIH Publication No. 95-1468 (National Institutes of Health, National Institute of Diabetes and Digestive and Kidney Diseases, 1995), 2nd ed.
3. N. F. Ray, M. Thamer, E. Gardner, J. K. Chan, and R. Kahn, *Diabetes Care* **21**, 296 (1998).
4. O. S. Khalil, *Clin. Chem.* **45**, 165 (1999).
5. J. T. Olesberg, L. Liu, V. Van Zee, and M. A. Arnold, *Proc. SPIE-Int. Soc. Opt. Eng.* **5325**, 11 (2004).
6. J. Wang, M. Maiorov, J. B. Jeffries, D. Z. Garbuzov, J. C. Connolly, and R. K. Hanson, *Meas. Sci. Technol.* **11**, 1576 (2000).
7. J. Wang, M. Maiorov, D. S. Baer, D. Z. Garbuzov, J. C. Connolly, and R. K. Hanson, *Appl. Opt.* **39**, 5579 (2000).
8. J. C. Nicolas, A. N. Baranov, Y. Cuminal, Y. Rouillard, and C. Alibert, *Appl. Opt.* **37**, 7906 (1998).
9. L. H. Xu, Z. F. Liu, I. Yakovlev, M. Y. Tretyakov, and R. M. Lees, *Infrared Phys. Technol.* **45**, 31 (2004).
10. R. D. May, *J. Geophys. Res.* **103**, 19161 (1998).
11. M. D. Brookes and A. R. W. McKellar, *J. Chem. Phys.* **109**, 5823 (1998).
12. C. R. Webster, G. J. Flesch, D. C. Scott, J. E. Swanson, R. D. May, W. S. Woodward, C. Gmachl, F. Capasso, D. L. Sivco, J. N. Bailargeon, A. L. Hutchinson, and A. Y. Cho, *Appl. Opt.* **40**, 321 (2001).
13. K. Namjou, S. Cai, E. A. Whittaker, J. Faist, C. Gmachl, F. Capasso, D. L. Sivco, and A. Y. Cho, *Opt. Lett.* **23**, 219 (1998).
14. P. Adamiec, A. Salhi, R. Bohdan, A. Bercha, F. Dybala, W. Trzeciakowski, Y. Rouillard, and A. Joulle, *Appl. Phys. Lett.* **85**, 4292 (2004).
15. P. Adamiec, F. Dybala, A. Bercha, R. Bohdan, W. Trzeciakowski, and M. Osinski, *Proc. SPIE-Int. Soc. Opt. Eng.* **4973**, 158 (2003).
16. F. Dybala, P. Adamiec, A. Bercha, R. Bohdan, and W. Trzeciakowski, *Proc. SPIE-Int. Soc. Opt. Eng.* **4989**, 181 (2003).
17. M. Bagley, R. Wyatt, D. J. Elton, H. J. Wickes, P. C. Spurdens, C. P. Seltzer, D. M. Cooper, and W. J. Devlin, *Electron. Lett.* **26**, 267 (1990).
18. H. Tabuchi and H. Ishikawa, *Electron. Lett.* **26**, 742 (1990).
19. H. Q. Le, G. W. Turner, J. R. Ochoa, M. J. Manfra, C. C. Cook, and Y.-H. Zhang, *Appl. Phys. Lett.* **69**, 2804 (1996).
20. H. Q. Le, G. W. Turner, J. R. Ochoa, M. J. Manfra, C. C. Cook, and Y.-H. Zhang, *Proc. SPIE-Int. Soc. Opt. Eng.* **3001**, 298 (1997).
21. C. Mermelstein, S. Simanowski, M. Mayer, R. Kiefer, J. Schmitz, M. Walther, and J. Wagner, *Appl. Phys. Lett.* **77**, 1581 (2000).
22. S. Simanowski, N. Herres, C. Mermelstein, R. Kiefer, J. Schmitz, M. Walther, J. Wagner, and G. Weimann, *J. Cryst. Growth* **209**, 15 (2000).
23. S. Simanowski, C. Mermelstein, M. Walther, N. Herres, R. Kiefer, M. Rattunde, J. Schmitz, J. Wagner, and G. Weimann, *J. Cryst. Growth* **227**, 595 (2001).
24. S. Simanowski, M. Walther, J. Schmitz, R. Kiefer, N. Herres, F. Fuchs, M. Maier, C. Mermelstein, J. Wagner, and G. Weimann, *J. Cryst. Growth* **202**, 849 (1999).
25. D. Mehuys, D. Welch, and D. Scifres, *Electron. Lett.* **29**, 1254 (1993).
26. M. Ahmed and M. Yamada, *J. Appl. Phys.* **95**, 7573 (2004).
27. S. G. Abdulrhmann, M. Ahmed, T. Okamoto, W. Ishimori, and M. Yamada, *IEEE J. Sel. Top. Quant. Electron.* **9**, 1265 (2003).
28. K. Petermann, *IEEE J. Sel. Top. Quant. Electron.* **1**, 480 (1995).
29. C. H. Grein, M. E. Flatté, J. T. Olesberg, S. A. Anson, L. Zhang, and T. F. Boggess, *J. Appl. Phys.* **92**, 7311 (2002).
30. W. H. Lau, J. T. Olesberg, and M. E. Flatté, *Phys. Rev. B* **64**, 161301 (2001).
31. J. T. Olesberg, W. H. Lau, M. E. Flatté, C. Yu, E. Altunkaya, E. M. Shaw, T. C. Hasenberg, and T. F. Boggess, *Phys. Rev. B* **64**, 201301 (2001).
32. S. A. Anson, J. T. Olesberg, M. E. Flatté, T. C. Hasenberg, and T. F. Boggess, *J. Appl. Phys.* **86**, 713 (1999).
33. M. E. Flatté, C. H. Grein, T. C. Hasenberg, S. A. Anson, D.-J. Jang, J. T. Olesberg, and T. F. Boggess, *Phys. Rev. B* **59**, 5745 (1999).
34. D.-J. Jang, M. E. Flatté, C. H. Grein, J. T. Olesberg, T. C. Hasenberg, and T. F. Boggess, *Phys. Rev. B* **58**, 13047 (1998).
35. J. T. Olesberg, S. A. Anson, S. W. McCahon, M. E. Flatté, T. F. Boggess, D. H. Chow, and T. C. Hasenberg, *Appl. Phys. Lett.* **72**, 229 (1998).
36. M. Rattunde, A. Huelsmann, J. Schmitz, G. Kaufel, J. Weber, M. Mikulla, and J. Wagner, *Proc. SPIE-Int. Soc. Opt. Eng.*, paper in press (2005).
37. J. Wagner, *Proc. SPIE-Int. Soc. Opt. Eng.*, paper in press (2005).
38. T. Swanson, *Photon. Spectra* **36**, 78 (2002).
39. I. F. Lealman, A. E. Kelly, L. J. Rivers, S. D. Perrin, and R. Moore, *Electron. Lett.* **34**, 2247 (1998).
40. B. Mason, J. Barton, G. A. Fish, L. A. Coldren, and S. P. DenBaars, *IEEE Photon. Technol. Lett.* **12**, 762 (2000).
41. C. A. Williamson, M. J. Adams, A. D. Ellis, and A. Borghesani, *Appl. Phys. Lett.* **82**, 322 (2003).
42. C.-F. Lin, Y.-S. Su, and B.-R. Wu, *IEEE Photon. Technol. Lett.* **14**, 3 (2002).